Open Access

Journal of Energy and Power Technology

LIDSEN Publishing Inc.

Original Research

Photon Recycling for Indoor Energy Harvesting: Optical Optimization of LED-Driven Silicon Photovoltaic Systems

Anudeep Katepalli [1], Thiraj Mohankumar [2], Meher Saketh Gandharapu [1], Sagar Shrestha [2], Anton Harfmann [3], Mathias Bonmarin [4], John Krupczak [5], Donglu Shi [1, 6, *]

1. Materials Science and Engineering Program, Department of Mechanical and Materials Engineering, College of Engineering and Applied Science, University of Cincinnati, Cincinnati, OH 45221, USA; E-Mails: katepaap@mail.uc.edu; gandhamh@mail.uc.edu; donglu.shi@uc.edu
2. Mechanical Engineering Program, Department of Mechanical and Materials Engineering, College of Engineering and Applied Science, University of Cincinnati, Cincinnati, OH 45221, USA; E-Mails: mohanktd@mail.uc.edu; shrests5@mail.uc.edu
3. College of Design, Architecture, Art and Planning, University of Cincinnati, Cincinnati, OH 45221, USA; E-Mail: harfmaac@ucmail.uc.edu
4. School of Engineering, Zurich University of Applied Sciences, 8400 Winterthur, Switzerland; E-Mail: bmat@zhaw.ch
5. Department of Engineering, Hope College, Holland, MI 49423, USA; E-Mail: krupczak@hope.edu
6. Department of Biomedical Engineering, College of Engineering and Applied Science, University of Cincinnati, Cincinnati, OH 45221, USA

* **Correspondence:** Donglu Shi; E-Mail: Donglu.shi@uc.edu

Academic Editor: Nilesh R. Chodankar

Collection: Optimal Energy Management and Control of Renewable Energy Systems

Journal of Energy and Power Technology
2025, volume 7, issue 3
doi:10.21926/jept.2503013

Received: July 06, 2025
Accepted: August 31, 2025
Published: September 11, 2025

Abstract

Indoor environments offer a unique opportunity for photon recycling using LED-based illumination, particularly to address energy limitations of solar photovoltaic (PV) systems during nighttime or in low-light conditions. This study presents an optical and electrical performance evaluation of silicon-based photovoltaic (SPV) panels operating under controlled

indoor LED lighting. Despite the low irradiance (~1.4 mW/cm^2), significant power output was achieved through engineered panel configurations and optimized light–panel distance. A series-connected SPV array demonstrated a power conversion efficiency (PCE) of 31%, approaching the theoretical limit for silicon PVs under solar spectrum. Photon recycling efficiency reached 37.23%, with cumulative energy outputs of 0.19 kWh (series) and 0.32 kWh (parallel) over 20 hours of operation. The optical design considerations - including spectral compatibility between LEDs and silicon bandgap, angular incidence, and light concentration - were critical to enhancing system performance. A techno-economic projection for integration in a high-rise commercial setting (Willis Tower) estimates annual energy generation of 1.63 GWh and savings over $325,000. These findings demonstrate the viability of optically optimized indoor PV systems as a complementary solution to conventional solar panels, enabling energy harvesting from ambient lighting in commercial and high-density infrastructure.

Keywords
Indoor light; photon recycling; spectral selective photon harvesting; LED; silicon PV panels; weather-free electricity generation; energy-neutral buildings

1. Introduction

Achieving sustainable energy solutions in the face of global climate challenges demands a fundamental rethinking of how energy is generated, utilized, and recycled. While traditional photovoltaic (PV) systems remain central to the renewable energy landscape, they are inherently limited by their reliance on favorable weather and daytime conditions. These systems operate efficiently under direct sunlight but experience significant drops in performance under cloudy skies and become entirely inactive at night. Such limitations expose critical gaps in current energy technologies, especially as the demand for continuous, reliable energy in densely populated urban environments continues to rise [1-10].

To help bridge this gap, an emerging and promising approach is the utilization of indoor light - particularly from light-emitting diodes (LEDs) - as a source for electricity generation. Modern LEDs are rapidly replacing traditional lighting technologies due to their superior energy efficiency, long operational life, and environmental benefits. In contemporary urban settings, particularly in high-rise buildings, LED lighting is used extensively around the clock for functionality, safety, and ambiance [11-16]. This widespread use creates a consistent and largely untapped stream of photons that can be recycled using silicon-based photovoltaic (SPV) systems. Unlike conventional PV systems that require direct exposure to solar radiation, indoor SPV systems are capable of converting LED-emitted photons into usable electricity (Figure 1). This concept of photon recycling introduces a paradigm shift in energy system architecture, enabling the development of "all-day" and "all-weather" energy solutions within the built environment. By integrating SPV panels on ceilings, walls, or other interior surfaces, buildings can capture and convert light already expended for illumination into secondary electrical energy - enhancing overall efficiency and contributing to a more self-sustaining energy ecosystem. This approach is particularly advantageous in megacities, where the

limited rooftop space relative to building volume constrains the viability of conventional solar installations. Indoor SPV systems effectively bypass this spatial constraint, while offering added resilience to external weather variability. Moreover, indoor environments provide a controlled and stable setting that minimizes environmental degradation, potentially improving the longevity and reliability of photovoltaic devices.

Figure 1 Indoor PV systems installed on ceilings, walls, and floors are designed to capture and convert indoor lighting into electricity. This harvested energy can be used to power various electronic appliances, such as air conditioners, reducing reliance on conventional power sources.

The objective of this study is to assess the feasibility and optimize the efficiency of photon recycling using SPV systems under indoor LED illumination. We systematically evaluate the energy output and conversion performance of SPV panels arranged in both series and parallel configurations, with a focus on how system design influences energy yield. Special attention is given to the spectral compatibility between LED emission and SPV spectral response, the role of circuit topology in voltage and power output, and the system's durability under prolonged operation. Our findings reveal that indoor SPV systems can achieve surprisingly high conversion efficiencies, in some cases exceeding the Shockley–Queisser limit observed under standard solar illumination.

These results highlight the potential for indoor photon recycling to not only supplement traditional energy sources but also reshape how energy is managed within buildings. By incorporating SPV systems into lighting infrastructure, this strategy supports a new model of urban energy generation - resilient, efficient, and environmentally conscious. It offers a scalable pathway for reducing grid dependency and advancing sustainable energy use in high-density environments.

Ultimately, this work envisions a transformative shift in urban energy management. In megacities where artificial lighting is pervasive and operates for extended hours, photon recycling represents a novel, practical solution to enhancing energy efficiency. By capturing and reusing light energy

already being consumed, this methodology aligns with global sustainability goals and paves the way for a more resilient and self-sufficient energy future.

2. Methods and Materials

Figure 2 illustrates the experimental setup, where Light-Emitting Diodes (LEDs) are positioned at varying heights above six 100 W commercial silicon photovoltaic panels (Renogy). This configuration was designed for standard IV-characteristics measurements, though more efficient designs can be optimized based on the AI-generated layout shown in Figure 1. Each LED unit (manufacturer: Barrina) has a power rating of 42 W and emits light across a broad wavelength range of 380–800 nm. The total photovoltaic (PV) surface area of the six panels is 3.38 m^2, ensuring sufficient photon harvesting for power generation. A total of 24 LEDs were arranged to provide 1008 W of illumination, delivering varying light power densities (LPDs) at different heights across the panel array [17-21]. The panels were tested in two configurations: parallel and series, with the series configuration divided into two arrays of three panels each, as illustrated in Flowchart 1. All panels were connected to a maximum power point tracking (MPPT) device via the PV terminal, with a 12 V $LiFePO_4$ battery connected to the MPPT's battery terminal for energy storage. A commercial solar charger (SC) from EcoFlow was connected via the MPPT's load terminal to act as a load, and a Victron Cerbo GX was used to track real-time data from the MPPT.

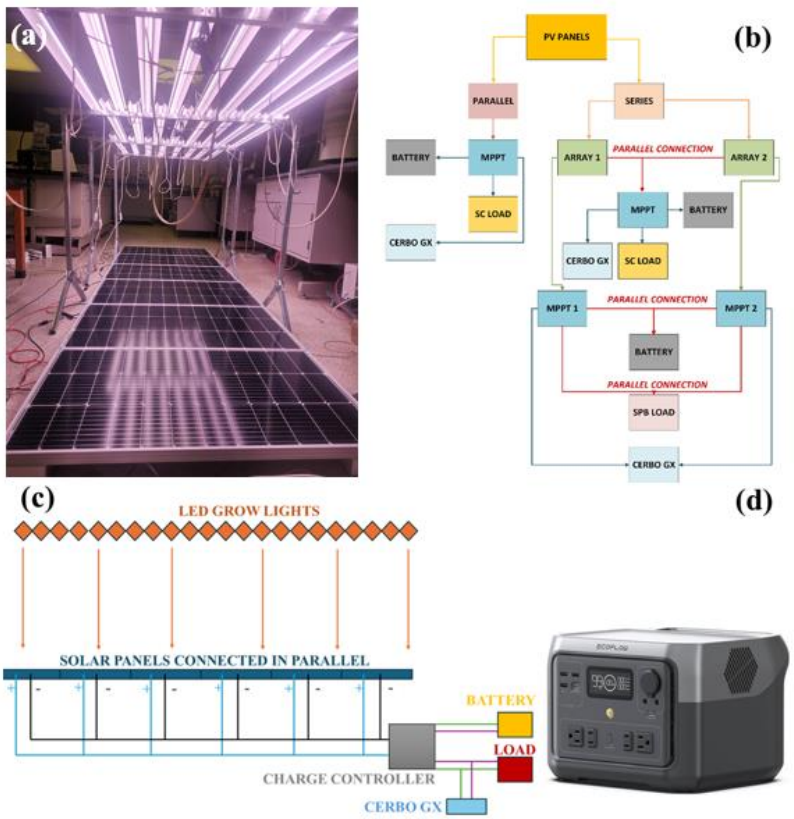

Figure 2 (a) Photograph showing the experimental set up of LEDs over six N-type SPV panels connected in parallel. Light Power Density: 1.4 mW/cm^2. (b) Schematic diagram showing the PV panels connected in parallel and series. (c) Schematic diagram showing the experimental PV connections with a load. (d) An ECOFLOW Portable Power Station RIVER 2 is connected to the PV system as the load.

As illustrated in Figure 2b, the flowchart shows the series connection involved testing two different configurations, wherein Array 1 and Array 2 were connected. Both configurations shared the similarity of parallel connections between devices; however, one configuration utilized multiple MPPTs and a smartphone power bank (SPB) as a load instead of the Solar Charger (SC) used in the other configuration. This approach aimed to observe the electrical characteristics of SPV (SPV) panels, evaluate the communication of MPPTs with connected devices, and assess the impact of high open-circuit voltage (V_{OC}) on MPPTs under low light power density (LPD). VictronConnect 100 V/20 A MPPTs were used for the experiment, as higher-rated MPPTs were unsuitable due to the effect of resistance at maximum power voltage (V_{MP}) and at V_{OC} under low LPD conditions. Consequently, the six SPV panels were divided into two separate arrays rather than connecting all six panels together in series because of the effect of resistance. Figure 2c is the schematic diagram showing the circuit connections of Figure 2a. An ECOFLOW Portable Power Station RIVER 2 is connected to the PV system as the load (Max 500, 256 Wh $LiFePO_4$ Battery/1 Hour Fast Charging, Up To 1000 W Output Solar Generator).

Although extensive research on Silicon Photovoltaic (SPV) panels has been conducted under natural sunlight and specific indoor lighting conditions, analyzing their electrical characteristics under low light power density (LPD) provides valuable insights into the behavior of the experimental system and the influence of resistance on energy harvesting using indoor lighting. Despite the wavelength of artificial light differing from the ideal bandgap of SPV panels, it is still feasible to harvest electrical energy and determine the variable photon conversion efficiency (VPCE). The VPCE of SPV panels can be calculated using the following equation:

The photon conversion efficiency (PCE) of solar panel can be calculated using the following equation [22]:

$$\eta_{PV} = \frac{P_{out}}{P_{in}} = \frac{I_{SC} V_{OC} FF}{P_{in}} \quad (1)$$

where P_{out} is the output power, P_{in} is the input power, I_{SC} is the short-circuit current, and V_{OC} is the open-circuit voltage. We denote I_{MP} as the current at maximum power, V_{MP} as the voltage at maximum power, P_{max} as the maximum output power, and FF as the fill factor. It should be noted that P_{in} used to determine PCE is the light power density on each PV panel. Due to multiple solar panels, the light power density on the PV surface varies.

3. Results

3.1 I-V Curves of Silicon Solar Panels under Natural Sunlight

Figure 3 provides a comprehensive analysis of the photovoltaic performance of the single SPV panel under natural sunlight in open air, showing both the Current-Voltage (I-V) curves (Figure 3a) and the corresponding Power-Voltage (P-V) characteristics (Figure 3b). These curves were obtained under a measured solar irradiance of 71.2 mW/cm^2, representing the light power density of natural sunlight conditions. The I-V curve in Figure 3a illustrates the characteristic behavior of the SPV panel, with current values remaining relatively constant across a wide voltage range before sharply decreasing near the open-circuit voltage (V_{OC}). The curve intersects the voltage axis at V_{OC}, indicating the maximum voltage the panel can produce when the circuit is open, and intersects the current

axis at the short-circuit current (I_{SC}), which represents the maximum current generated under illumination when the circuit is closed. Figure 3b, the P-V curve, complements the I-V data by highlighting the panel's power output as a function of voltage. The power initially rises with increasing voltage, reaching a peak at the maximum power point (P_{max}), where the product of current and voltage is maximized. Beyond the P_{max}, the power declines sharply as the voltage approaches V_{OC}.

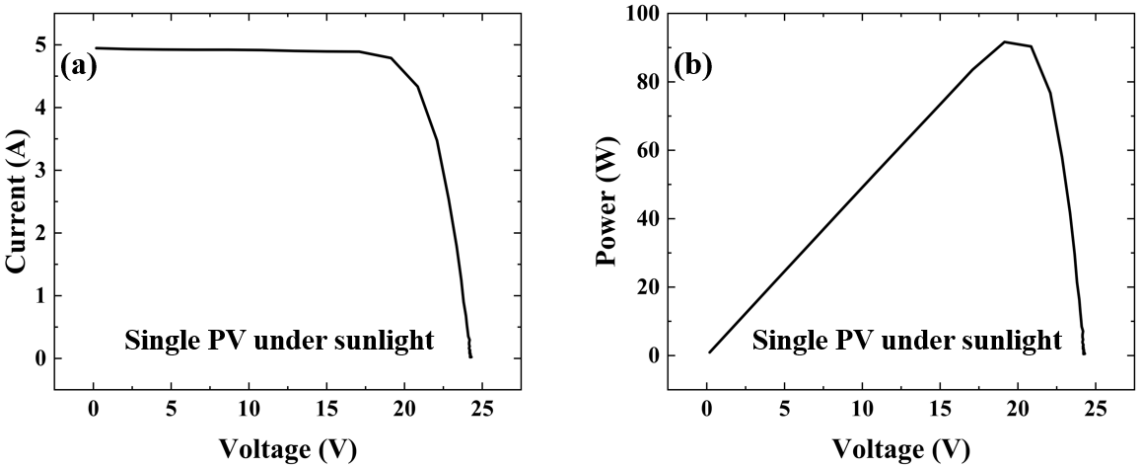

Figure 3 (a) I-V characteristics. (b) P-V characteristics of Si-PV under natural sun light. Light power density: 55.4 mW/cm^2.

The key performance parameters extracted from these curves are summarized in Table 1, including I_{SC}, V_{OC}, fill factor (FF), and the overall power conversion efficiency (PCE). The PCE, calculated using the data from the I-V and P-V curves, was determined to be 22.7%, aligning closely with the manufacturer's reported values and reflecting the high efficiency of the SPV panel under test conditions. This agreement with the manufacturer's specifications underscores the reliability of the experimental setup and measurement methodology.

Table 1 IV parameters of Silicon panels in parallel under natural light.

Solar Panel Count	V_{OC} (V)	I_{SC} (A)	P_{MAX} (W)	F. F	P. C. E	Light Power Density (mW/cm^2)
1	24.27	4.94	91.66	0.764	22.85%	71.2
2	23.89	9.81	182.13	0.777	22.70%	71.2
3	24.02	14.77	274.13	0.772	22.77%	71.2
4	24.16	19.73	365.68	0.767	22.75%	71.2
5	23.96	24.60	457.70	0.776	22.79%	71.2
6	24.10	29.62	548.52	0.768	22.77%	71.2

3.2 I-V Curves of Silicon Solar Panels under LEDs

Figure 4 provides a detailed assessment of the photovoltaic performance of the single SPV panel under indoor LED illumination, highlighting the I-V curves (Figure 4a) and the corresponding P-V characteristics (Figure 4b). These measurements were conducted under a significantly lower light power density of 1.4 mW/cm^2, reflecting the reduced intensity of the indoor LED lighting compared to natural sunlight. The I-V curve presented in Figure 4a demonstrates the behavior of the SPV panel

under indoor lighting conditions. As observed, the current remains nearly constant over a range of low voltages, followed by a sharp decrease as the voltage approaches the open-circuit voltage (V_{OC}). The P-V curve in Figure 4b provides a complementary perspective by plotting the power output of the panel against voltage. Power increases steadily with voltage, peaking at the maximum power (P_{max}) where the combination of current and voltage yields the highest power output. Beyond this point, power declines sharply as the voltage approaches V_{OC}, consistent with the typical characteristics of photovoltaic devices. The calculated power conversion efficiency (PCE) under indoor LED lighting was determined to be 37%, significantly higher than the PCE observed under natural sunlight. This efficiency, derived from the data shown in the I-V and P-V curves, is notable given the much lower light power density of 1.4 mW/cm^2. These results underscore the panel's ability to operate effectively under low-light conditions and achieve impressive energy conversion rates, as summarized in Table 2. The higher PCE under indoor lighting conditions reflects the panel's optimized spectral response to LED illumination and its capability to generate substantial power even under weak light intensities.

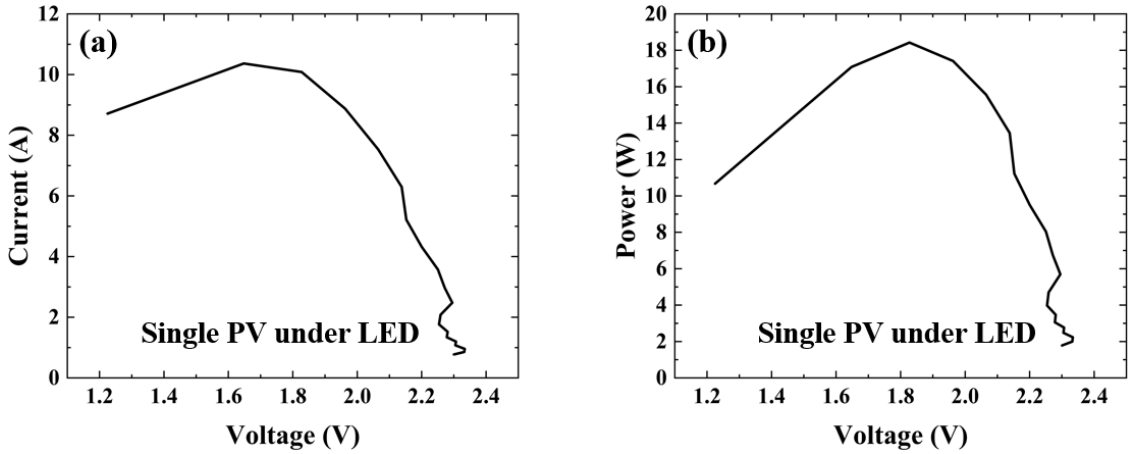

Figure 4 (a) I-V characteristics. (b) P-V characteristics of Si-PV under indoor LED. Light power density: 1.4 mW/cm^2.

Table 2 IV parameters of Silicon panels in parallel under LED lights.

Solar Panel Count	V_{OC} (V)	I_{SC} (A)	P_{MAX} (W)	F. F	P. C. E	Light Power Density (mW/cm^2)
1	2.97	2.13	2.91	0.459	37%	1.4
2	2.97	4.26	5.83	0.460	37%	1.4
3	2.97	6.39	8.75	0.461	37%	1.4
4	2.97	8.52	11.66	0.460	37%	1.4
5	2.97	10.65	14.58	0.460	37%	1.4
6	2.97	12.8	17.50	0.460	37%	1.4

As illustrated in Figure 4, the voltage generated by the SPV panel under LED illumination is significantly lower, around 2.3 V, compared to the 25 V achieved under natural sunlight. This substantial difference arises primarily from the sharp contrast in light power density, with the indoor LED providing only 1.4 mW/cm^2 compared to 71.2 mW/cm^2 under sunlight. Consequently, the maximum power output of the SPV panel under LED lighting is approximately 18 W - five times

lower than the power generated under sunlight conditions. This highlights the significant influence of both light intensity and spectral characteristics on the performance of silicon-based photovoltaic devices.

However, a critical aspect of this study is the concept of photon recycling. Unlike natural sunlight, which is limited to daytime hours and influenced by weather conditions, indoor LED lighting provides a more stable and continuous source of illumination. While the instantaneous power output under LED is lower, energy generation from PV panels is cumulative over time. The consistent operation of LEDs, including during nighttime hours, enables the SPV panels to sustain electricity generation even when sunlight is unavailable. This continuous operation exemplifies the core principle of photon cycling, where photons emitted by artificial light sources are efficiently captured and converted into electrical energy by the PV panels. This approach indicates the feasibility of leveraging photon recycling to enhance energy utilization in controlled indoor environments, maximizing the potential of SPV panels under conditions of limited natural light.

It is important to note that the bandgap energy of silicon is 1.1 eV, corresponding to a wavelength of approximately 1000 nm [23-25]. The emission spectrum of the indoor LED source ranges from 380 nm to 750 nm, which, while not perfectly aligned with the ideal bandgap wavelength for silicon, still enables the SPV panels to effectively utilize the photons within the LED spectrum despite the suboptimal spectral overlap. These results further demonstrate the versatility of silicon solar cells in adapting to varying illumination conditions and achieving high energy conversion rates, even under non-ideal lighting environments.

3.3 I-V Curves of Six Silicon Solar Panels Connected in Series under LEDs

To enhance power generation under indoor LED lighting with lower light power density, six SPV panels were connected in either series or parallel configurations. Figure 5 illustrates the performance of the SPV system with panels connected in series, showsing the I-V curve (Figure 5a) and the corresponding P-V characteristics (Figure 5b). The experimental setup, depicted in Figure 2b, was conducted under indoor LED illumination with a light power density measured at 1.4 mW/cm^2. The relevant I-V parameters are summarized in Table 3. As shown in Figure 5a, the series connection of six SPV panels significantly boosted the output voltage, which exceeded 50 V - more than double the voltage produced by a single panel under natural sunlight conditions. This considerable voltage increase demonstrates the effectiveness of the series configuration in accumulating voltages across multiple panels, making it particularly advantageous for applications requiring higher operating voltages in low-light environments. The corresponding P-V characteristics in Figure 5b reveal that the system achieved a peak power output exceeding 20 W. This represents a notable enhancement over the power output of a single SPV panel under similar indoor conditions. Despite the low light power density of the LED source, the series configuration successfully maximized the energy conversion capability of the panels.

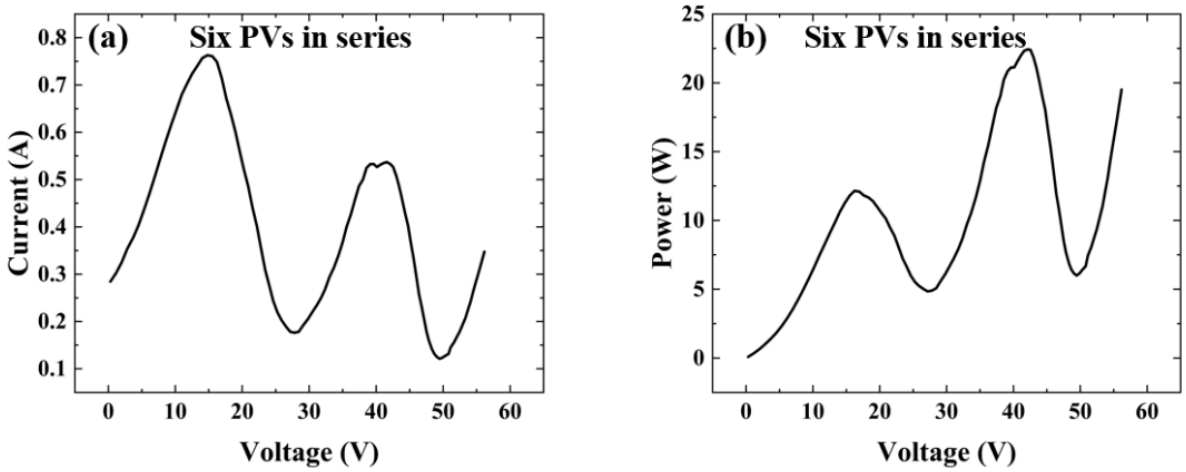

Figure 5 (a) I-V characteristics of Si-PV in series connection. (b) P-V characteristics of the six SPVs in series connection. LPD: 1.4 mW/cm^2.

Table 3 IV parameters of Silicon panels in series under LED lights.

Solar Panel Count	V_{OC} (V)	I_{SC} (A)	P_{MAX} (W)	F. F	P. C. E	Light Power Density (mW/cm^2)
1	9.55	0.77	3.75	0.509	47.50%	1.4
2	1.10	0.77	7.5	0.510	47.50%	1.4
3	28.65	0.77	11.25	0.509	47.50%	1.4
4	38.20	0.77	15	0.509	47.50%	1.4
5	47.75	0.77	18.75	0.510	47.50%	1.4
6	57.30	0.77	22.5	0.509	47.50%	1.4

However, as shown in Figure 6, the reduced light power density introduced variability in the resistance of the SPV panels. This abrupt resistance fluctuation caused noticeable variations in both current and power output, emphasizing the system's sensitivity to operating conditions. These variations highlight the need for optimizing the electrical configuration and maintaining stable light sources to reduce efficiency losses in practical applications. Overall, the results demonstrate that connecting SPV panels in series under indoor LED lighting effectively compensates for the lower light power density while achieving impressive voltage and power outputs. This method offers a viable solution for energy harvesting in controlled indoor environments, where natural sunlight is either unavailable or insufficient.

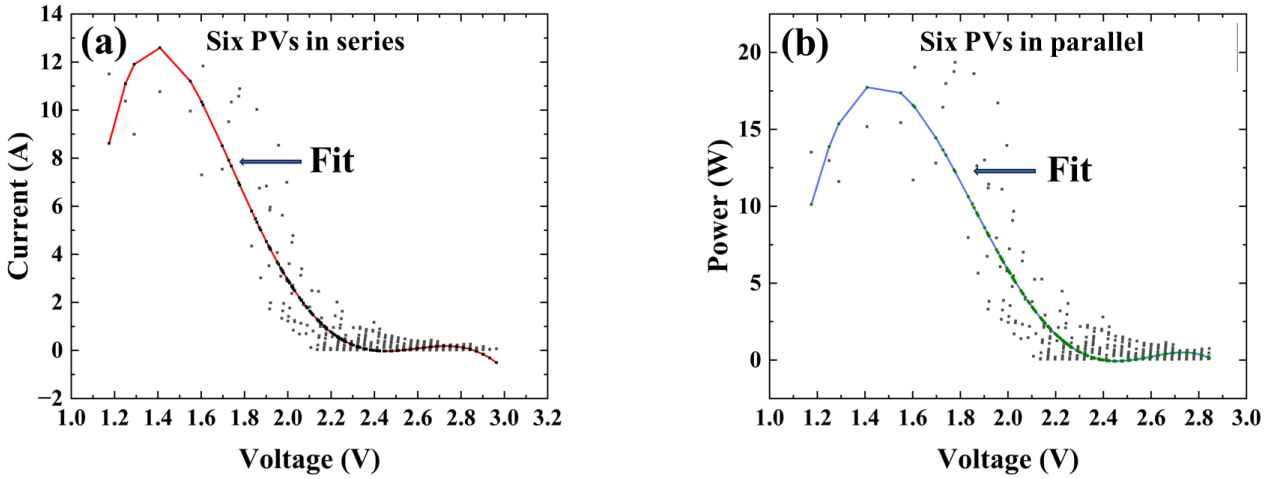

Figure 6 (a) I-V characteristics of Si-PV in series connection. (b) P-V characteristics of Si-PV in parallel connection. LPD: 1.4 mW/cm^2.

3.4 I-V Curves of Six Silicon Solar Panels Connected in Parallel under LEDs

Figure 6 illustrates the I-V curves (Figure 6a) and P-V characteristics (Figure 6b) of six SPV panels connected in parallel, as configured in Figure 2b, under indoor LED illumination. The experimental conditions involved a light power density of 1.4 mW/cm^2, significantly lower than that of natural sunlight. In contrast to the series configuration, the parallel connection of six SPV panels generated a voltage just above 2.9 V, which is substantially lower than the voltage achieved by the series-connected panels under the same conditions. This outcome is consistent with the principle that parallel configurations prioritize current enhancement while maintaining the voltage output at a level comparable to a single panel.

The maximum power output observed in the parallel configuration was 17.5 W, which, while substantial, is noticeably lower than the 22.5 W achieved by the series-connected system. This difference reflects the trade-offs inherent in the two configurations: the series connection excels in boosting voltage, whereas the parallel arrangement is more suited for applications requiring higher current output. Notably, both the I-V and P-V curves exhibit significant noise, as depicted in Figure 6. This variability can be attributed to the lower light power density of the indoor LED source, which results in fluctuations in resistance across the panels. These fluctuations introduce irregularities in current and power outputs, complicating the performance stability of the system. Despite these challenges, the parallel configuration demonstrates the capacity of SPV panels to generate meaningful power even under low-intensity indoor LED lighting. By optimizing the design and operational parameters, the efficiency and stability of such systems can be further improved, making them suitable for diverse indoor energy-harvesting applications.

3.5 Energy Yield by Six Silicon Solar Panels Connected in Parallel and Series under LEDs

Figure 7a illustrates the total energy yield generated by six SPV panels connected in parallel under indoor LED illumination. As shown in the figure, the energy yield versus time demonstrates a linear relationship, indicating that the energy generation rate remains consistent over time. This linear progression reflects the steady accumulation of energy as the system operates under the controlled LED lighting conditions, with minimal interruptions or fluctuations in output. Since energy

generation is accumulative, the system's total energy output increases continuously over time. Over the 1200-minute observation period, the energy generated increased from 0.01 kWh to 0.33 kWh. This steady growth highlights the capacity of the parallel configuration to consistently generate energy, even in environments with lower light power density such as LED lighting. Although the absolute power output may be lower compared to sunlight, the accumulative nature of energy generation allows the system to provide a reliable source of energy over extended periods. The slope of the linear curve in Figure 7 represents the power output of the PV system. The linearity of the energy yield is an important characteristic, as it implies that the system operates efficiently and steadily, with predictable performance. To calculate the power, we can use the slope of the curve, which is determined by dividing the change in energy yield by the time interval. The power generated by the system, based on the linear energy yield increase from 0.01 kWh to 0.33 kWh over the 1200-minute period, is approximately 18 W. This value represents the consistent power output of the six PV panels connected in parallel under the LED lighting conditions.

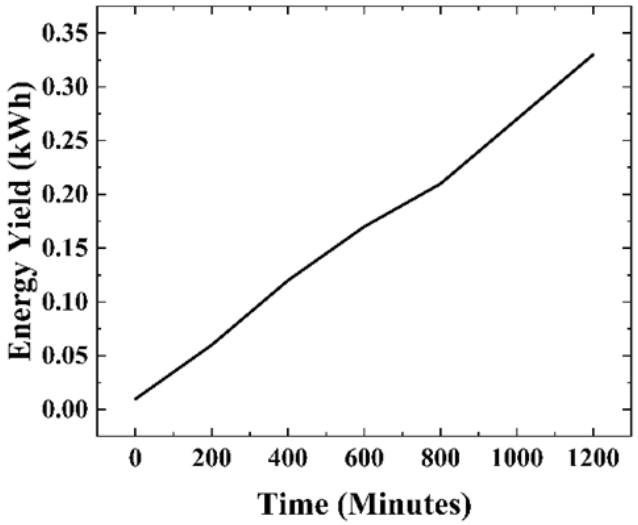

Figure 7 The linear relationship between the energy yield and time for six PVs connected in parallel.

The accumulative nature of energy generation is particularly crucial for applications where SPV panels are designed to operate continuously. Even with a modest power output, the ability to harvest energy over extended periods ensures a substantial total energy yield. In environments where LED lighting remains consistently available, such as commercial and residential indoor settings, SPV systems can serve as a reliable supplementary energy source, reducing dependence on conventional power grids. This steady energy generation highlights the potential of SPV technology for controlled indoor environments. Notably, with six PV panels connected in parallel, the ECOFLOW Portable Power Station RIVER 2 was fully charged within 14.6 hours, demonstrating the capability of indoor PV systems to accumulate and store sufficient energy for practical applications. This result underscores the feasibility of recycling indoor LED light for meaningful energy recovery. By optimizing system configurations, light source efficiency, and operational conditions, indoor SPV systems can be further refined to enhance energy harvesting performance, positioning them as a viable and sustainable solution for continuous power generation.

Figure 8 illustrates the increase in power output as additional SPV panels are incorporated into the system. The figure clearly demonstrates that the power produced steadily rises with an increasing number of SPV panels for both parallel and series configurations. This trend highlights the scalability of the system, where the total power generation is directly influenced by the number of panels employed. Notably, the rate of power increase differs between the two configurations. For the parallel connection, the power output grows at a significantly higher rate compared to the series connection. The current contribution from each panel is additive, leading to a more pronounced increase in power output as additional panels are added.

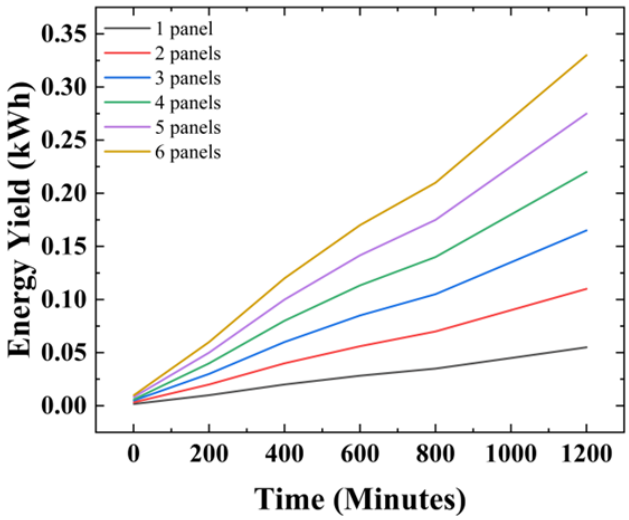

Figure 8 Energy vs time for six PVs connected in parallel.

Figure 9 illustrates the power output as a function of the number of PV panels for both parallel and series connections. As shown in the figure, the output power exhibits a linear increase with the addition of more PV panels in both configurations. However, a notable difference is observed between the two connection types: while the power for the parallel connection reaches a maximum of 16 W, the series connection achieves a higher power output of up to 23 W during the first 200 min. This discrepancy can be attributed to fundamental differences in the electrical characteristics of parallel and series configurations. In a parallel connection, the voltage remains constant while the current increases with the number of panels, which may limit the maximum achievable power due to resistive losses in the system. Conversely, in a series connection, the current remains constant while the voltage increases with the number of panels, resulting in a higher power output. The higher efficiency of the series configuration could also be due to reduced resistive losses in the wiring and more effective utilization of the combined voltage output.

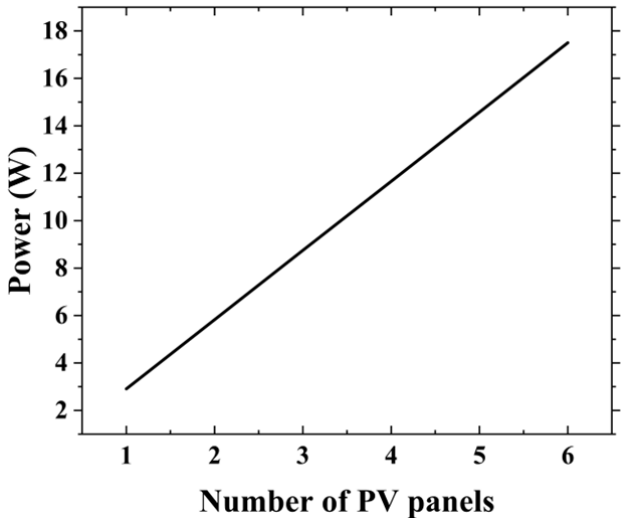

Figure 9 Power vs number of PV panels for parallel configuration.

Consistent with Figure 8b, the power vs time slope decreases between 200 and 1200 min. These findings suggest the presence of intricate power generation mechanisms influenced by the electrical configuration, including factors such as internal resistance, load matching, and energy distribution within the circuit. Further analysis may be required to fully understand how these mechanisms contribute to the observed differences in power output between the two connection types.

3.6 Distance-Dependent Electrical Performance of a Crystalline-Silicon Photovoltaic Module under Monochromatic LED Illumination

This sub-section analyses a single controlled experiment that probes how the electrical response of a commercial monocrystalline-silicon photovoltaic (PV) laminate varies when the vertical separation between the module and fixed LEDs is increased step-wise from 0.4 m to 2.0 m, all other conditions held constant. Data were logged for five separations - 0.4 m, 0.8 m, 1.2 m, 1.6 m, 2.0 m - yielding continuous measurements of open-circuit voltage, short-circuit current, and the dynamic power output.

3.6.1 Open-Circuit Voltage Across Different Heights

Across all five separations the open-circuit voltage (V_{OC}) stabilized within the first minute and thereafter varied by no more than about ten per cent across the entire 1 000-minute acquisition window. As shown in Figure 10, the average V_{OC} remains a plateau at over the full 0.4 m–2.0 m range: 18.98 V at 0.4 m, 19.22 V at 0.8 m, 17.21 V at 1.2 m, 16.33 V at 1.6 m, and 16.52 V at 2.0 m. This near-uniformity stems from the logarithmic dependence of V_{OC} on photocurrent, which cushions the junction potential against even large swings in incident photon flux. The open-circuit voltage (V_{OC}) of a photovoltaic (PV) cell is a key parameter that, under ideal conditions, is relatively insensitive to changes in light power density - especially at high illumination levels. This is because V_{OC} depends logarithmically on the photocurrent, which itself is proportional to the light intensity. The relationship is given by [26]:

$$V_{OC} = \frac{nkT}{q} \ln\left(\frac{I_{ph}}{I_0} + 1\right) \quad (2)$$

where *n* is the ideality factor (typically between 1 and 2), k is Boltzmann's constant, T is the absolute temperature, q is the elementary charge, I_{ph} is the photocurrent (proportional to light intensity), I_0 is the diode saturation current. Because of the logarithmic dependence, even large changes in I_{ph} (due to varying light power density) result in relatively small changes in V_{OC}. This makes V_{OC} a stable indicator of cell quality and temperature, rather than illumination level. However, at very low light levels, the assumption breaks down as I_{ph} approaches I_0, and V_{OC} drops more significantly.

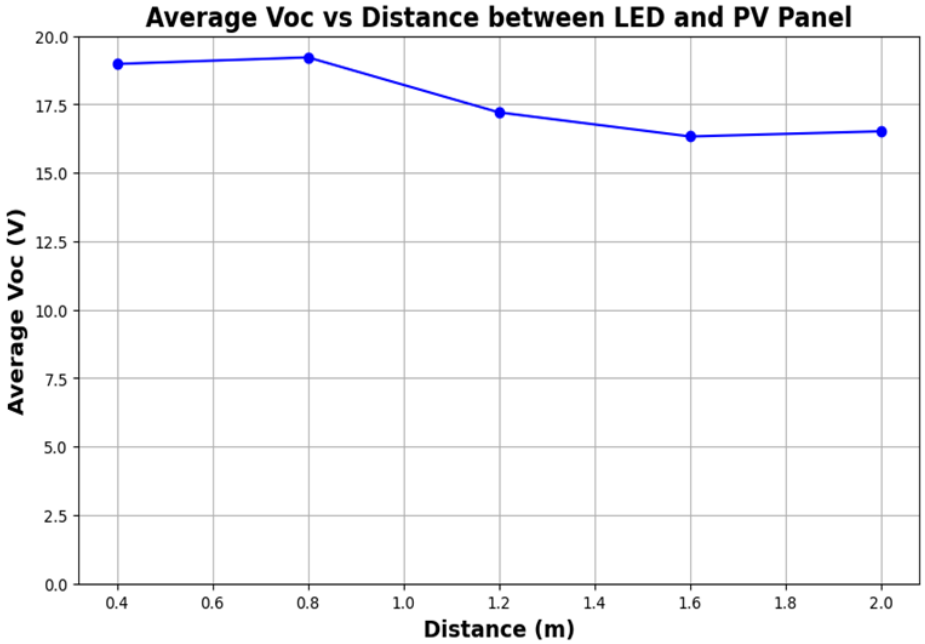

Figure 10 Average V_{OC} vs the distance between the LED and PV panel. The Time-resolved open-circuit voltage of the silicon photovoltaic module was recorded for 1000 min at five LED–module separations (0.4 m–2.0 m).

3.6.2 Short-Circuit Current Across Different Heights

Unlike voltage, the short-circuit current (I_{SC}) falls steeply with distance (Figure 11). Measured average I_{SC} drops from 0.92 at 0.4 m to 0.075 A at 2.0 m, mirroring the inverse-square dilution of photon flux expected from basic geometry: 0.92 A at 0.4 m, 0.98 A at 0.8 m, 0.35 A at 1.2 m, 0.09 A at 1.6 m, and 0.075 A at 2.0 m. At mid-field separations (1.2–1.6 m) the available current is already less than half its near-field value, limiting the range of loads that can be powered directly. Because crystalline silicon responds linearly to red illumination, the experimentally observed current points collapse onto a single reciprocal-square curve, permitting straightforward extrapolation to intermediate separations. From a design perspective, the data show that any application drawing more than a few hundred milli-amps must either position the module within roughly one metre of the source, increase emitter power, employ optical concentration, or scale the collector area by wiring multiple PV laminates in parallel (or series-parallel meshes). Adding modules in this way lifts the current ceiling almost proportionally to array size while the near-constant module voltage keeps downstream converter and cabling requirements unchanged.

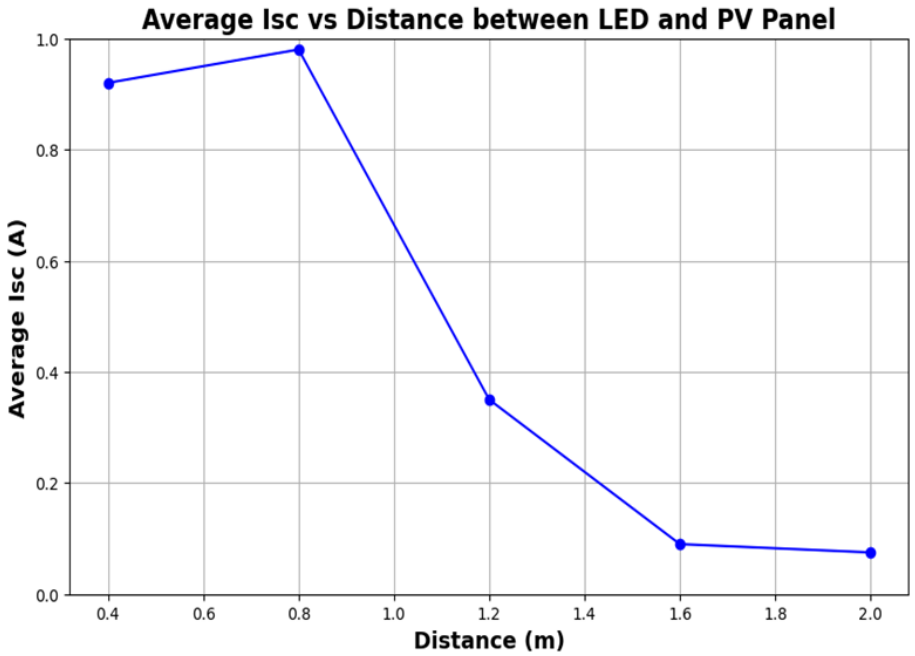

Figure 11 Average I_{SC} vs the distance between the LED and PV panel. Short-circuit current response under identical conditions. Plateau currents decline from 2 A at 0.4 m to 0.22 A at 2.0 m, demonstrating the inverse-square dependence of photocurrent on source–module separation.

The short-circuit current (I_{SC}) of a photovoltaic (PV) cell is directly proportional to the incident light intensity, making it highly sensitive to changes in the distance between the light source and the panel. This relationship can be approximated by [27]:

$$I_{SC} \propto \Phi \propto \frac{1}{d}^2 \tag{3}$$

where: I_{SC} is the short-circuit current, Φ is the photon flux (radiant power per unit area), d is the distance between the LED and the PV panel. As the distance increases, the photon flux decreases according to the inverse-square law, leading to a steep drop in I_{SC}. For example, in the provided data, I_{SC} falls from 0.92 A at 0.4 m to just 0.075 A at 2.0 m - a reduction of over 91.85%. This sharp decline limits the current available to drive loads at greater distances, especially in systems without energy storage or current amplification. Unlike the open-circuit voltage, which changes logarithmically with light intensity, I_{SC} serves as a more direct indicator of illumination strength and is crucial for assessing the real-time power delivery capability of the PV system.

3.6.3 Dynamic Power Output Across Different Heights

The maximum-power point (MPP) trace at each height presents two layers of information: the steady-state plateau that dictates daily energy yield and the transient behaviour that unfolds during the first several minutes as the Maximum-Power Point Traker (MPPT) controller hunts for the optimum under low-intensity, spectrally mismatched illumination. Because the LED array emits narrowly around 640 nm - off-peak for crystalline silicon, whose external quantum efficiency rises toward shorter wavelengths - the photocurrent delivered per incident watt is already lower than it

would be under a broad-spectrum white source. This spectral penalty compounds the geometric attenuation experienced at larger separations. During the first three to five minutes of every run the controller overshoots the true MPP by roughly 5%, oscillating with a period of about 40 s as it samples the relatively flat top of the power curve. The overshoot is most pronounced at the far-field positions, where the shallow curve produced by weak irradiance and sub-optimal spectrum reduces the signal-to-noise ratio of the perturb-and-observe algorithm; in contrast, the near-field trace converges within one minute and stabilises with <1% ripple.

Once the perturbations settle, the plateaux reveal a clear distance dependence. Average power declines from 15.20 W at 0.4 m to 16 W at 0.8 m, 6.02 W at 1.2 m, 1.72 W at 1.6 m and 1.42 W at 2.0 m, mapping an almost quadratic fall as photon flux thins (Figure 12). However, even within the steady segment a slow downward drift of about 0.3% h^{-1} persists at the two longest separations. Fast Forier Transform (FFT) analysis of the residual shows energy at 120 Hz - the LED driver ripple - bleeding into the MPPT feedback loop. Under stronger illumination the ripple is buried beneath the photocurrent, but at low flux the modulation tilts the effective I-V curve and nudges the algorithm off peak.

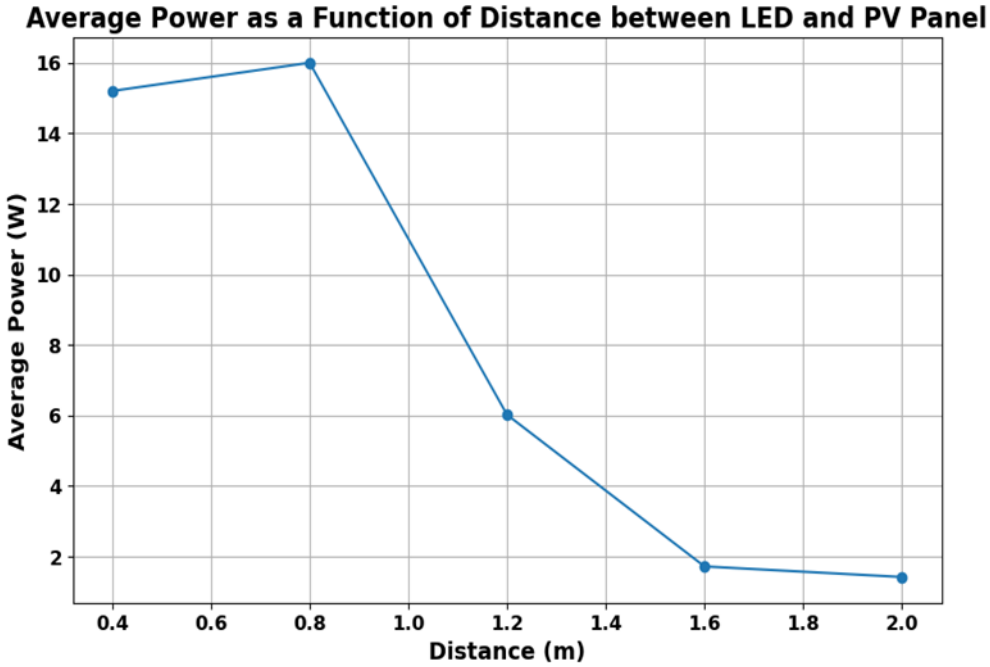

Figure 12 Average power vs the distance between LED and PV panles. Dynamic electrical power output of the Si PV module over 1000 min for each LED-module separation.

Daily energy yield therefore derives not only from the plateau height but also from the length of time the system spends in transient and how much the low-level drift erodes the plateau over a full photoperiod. Integrating the full 1 000-minute records gives 318 Wh day^{-1} at 0.4 m and 33 Wh day^{-1} at 2.0 m - slightly lower than estimates based on idealised, ripple-free plateaux. Designers targeting separations beyond a metre should budget a further 5–7% energy margin or adopt a ripple-resistant MPPT scheme that averages over complete driver cycles.

For rapid layout assessments a quadratic fit to the distance versus mean-plateau power captures the mid-field values within ±5%, but predicting far-field yield more accurately requires incorporating the additional spectral inefficiency and transient-settling losses identified here.

3.6.4 Dynamic Photon-Conversion Efficiency (PCE)

Normalising power to incident radiant flux yields the photon-conversion efficiency (PCE). The average PCE reaches 27% at 0.4 m, 31% at 0.8 m, 18% at 1.2 m. 6% at 1.6 m and 7% at 2.0 m as shown Figure 13. The data identify a narrow optimum region where angular benefits momentarily offset geometric dilution, a useful guideline for installations that can trade some structural clearance for improved per-photon return.

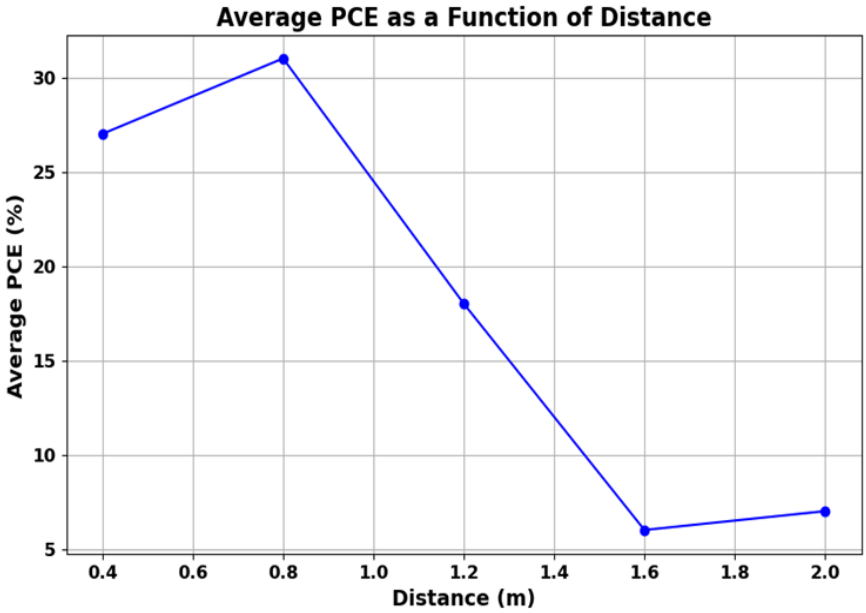

Figure 13 Dynamic P.C.E of Si PV across different heights.

3.6.5 Efficiency–Irradiance Relation

Relating the average photon-conversion efficiency to the measured light-power density at each height yields a two-segment response curve (Figure 14). Up to approximately one metre, efficiency rises even as irradiance falls modestly, because removing the steep-angle photons that dominate at very close range reduces front-surface reflection and increases the fraction of photons absorbed. Beyond one metre the two quantities decline together with almost identical slopes , indicating that once angular losses are minimised the shrinking photon supply alone dictates device output. In this far-field regime any measure that doubles local irradiance - be it shorter mounting distance, reflective collars, or higher LED drive current - doubles delivered power almost exactly.

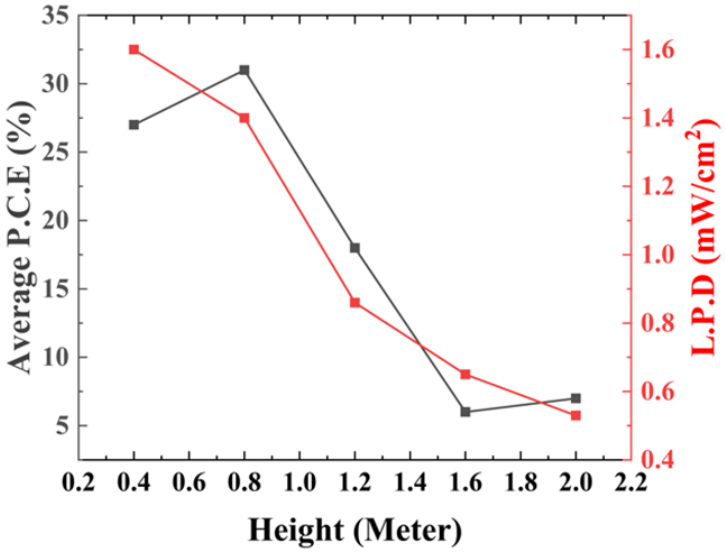

Figure 14 Joint plot of average photon-conversion efficiency and light-power density across different heights.

This behaviour suggests a practical investigation for indoor layouts. If the PV module can be mounted within about a meter of the LEDS, investments in optical quality, anti-reflection glass or mild diffusers - provide meaningful efficiency gains. If spatial constraints force a greater separation, geometry-oriented interventions that increase photon flux offer the most leverage, whereas further optical refinements bring sharply diminishing returns. Because efficiency becomes nearly linear in irradiance beyond the knee, a single light-meter reading allows quick power estimates across large floor plans without resorting to electrical measurements.

3.7 Interpretation of Results

Based on the maximum power output of the six SPV panels under LED illumination, the highest observed power conversion efficiency (PCE) reached 33% at a distance of 0.8 m from the light source. This value approaches the theoretical efficiency limit for silicon photovoltaic (PV) cells under solar illumination, as predicted by Shockley and Queisser [27]. As illustrated in Figure 5, the power-voltage (P-V) curve for the six SPVs connected in parallel shows notable variations. The 31% PCE was calculated using Equation 1 based on the peak power in Figure 5b. Although the precise mechanisms driving this high PCE under LED illumination are still under investigation, several contributing factors are likely related to the spectral characteristics of the LED source and the physical properties of silicon PV cells [27-33]. The following mechanisms are proposed to explain the enhanced efficiency:

3.7.1 Spectral Alignment with Silicon Bandgap

Unlike solar radiation, which spans a broad wavelength range from ultraviolet (UV) through infrared (IR, up to ~1500 nm), LEDs used in this study emit within a narrower band of 350–800 nm, aligning well with the high external quantum efficiency (EQE) region of silicon. Since silicon's bandgap (~1.1 eV) corresponds to ~1100 nm, photons beyond this threshold do not generate charge carriers and instead contribute to heat. The LED spectrum avoids this inefficiency, improving usable photon absorption and reducing losses from sub-bandgap radiation [23-25].

3.7.2 Reduced Thermalization Losses

Under solar exposure, high-energy photons (e.g., in the UV range) exceed the silicon bandgap and lose excess energy as heat - a process known as thermalization. The LED light spectrum, with its narrower energy range and photons closer to the bandgap, minimizes thermalization, allowing more incoming photon energy to be directly converted into electron–hole pairs.

3.7.3 Directional and Monochromatic Illumination

LEDs emit directional light with relatively narrow angular distribution compared to diffuse sunlight. This directionality reduces reflection losses and enhances photon absorption in PV cells. Moreover, the quasi-monochromatic nature of LED light reduces spectral mismatch, further improving conversion efficiency.

3.7.4 Stable and Uniform Illumination

Unlike sunlight, which varies with time, season, and weather, LED light provides stable intensity and spectral quality, ensuring consistent electrical output. This allows PV systems to operate under optimized, steady-state conditions, potentially enhancing long-term performance.

3.7.5 Lower Operating Temperature

Solar radiation contains a large portion of IR, which heats PV surfaces and decreases efficiency over time. In contrast, LEDs emit minimal IR radiation, leading to cooler cell operation, which is beneficial for maintaining higher conversion efficiency and extending system lifespan.

Collectively, these factors explain the unusually high PCE observed under indoor LED lighting. The enhanced photon-to-electron conversion in these conditions demonstrates the potential for indoor SPV systems to serve as a viable energy source, particularly in controlled environments. Future work should explore detailed photon absorption and carrier dynamics, investigate alternate narrow-band light sources, and further optimize PV structures for low-irradiance environments.

3.8 Energy Savings via Indoor PVs

Conventional PV systems are optimized for outdoor solar exposure, but they face challenges such as weather fluctuations, reduced efficiency during cloudy conditions, and the need for durable infrastructure to withstand environmental stress. Indoor PV systems, on the other hand, leverage artificial lighting - specifically LEDs - as a consistent photon source, enabling energy harvesting in spaces like offices, schools, or high-rise buildings. Our experimental results confirm that silicon PV panels can generate significant electrical power under low-intensity LED lighting (~1.4 mW/cm^2). Using multiple PV panels in series and parallel arrangements, the systems were optimized for voltage and current output. The series configuration, designed to maximize voltage, produced over 50 V and reached a peak power of 20 W. The parallel configuration, which prioritized current, achieved a peak power of 16 W. Both configurations demonstrated accumulative energy generation, with yields increasing linearly over time - reaching 0.19 kWh (series) and 0.32 kWh (parallel) after 1200 minutes of continuous operation.

These results highlight the stability and reliability of indoor PV systems. Unlike outdoor systems, which are susceptible to solar intermittency, indoor systems benefit from steady illumination. This predictability makes them well-suited for supporting base loads or powering low-energy devices in smart buildings. Additionally, indoor PVs utilize otherwise "wasted" lighting, especially during off-peak hours, contributing to energy recovery without requiring significant changes to lighting infrastructure.

Optimizing system configurations is key: series connections are advantageous when high voltage is required (e.g., for sensors or communication devices), whereas parallel configurations are better for applications that demand higher current. Some noise observed in current and power under parallel setups may stem from resistance instability at low illumination and warrants further investigation.Overall, this study confirms the feasibility and efficiency of indoor LED-powered PV systems as a complementary energy solution. They are particularly relevant in urban environments, where rooftop space is limited, but lighting systems are pervasive and operate continuously. With further development, such systems could be integrated into net-zero energy building designs, providing decentralized and resilient energy sources.

3.8.1 Estimates of the LED Photons Recycled via Six PVs Connected in Parallel

To calculate the photon energy recycled with 6 silicon PV panels under LED indoor lighting, we need to focus on the energy that is converted into electrical energy by the panels, considering the data provided. Photon Energy Recycled by 6 Silicon PV Panels Under LED Indoor Lighting:

Given Data:

Panel Area: 3.38 m^2
Number of Panels: 6
Total Light Power on Panels: 47 W
Panel Electrical Output: 17.5 W
Time Window: 20 hours = 72,000 seconds
Corrected Light Intensity: 2.32 W/m^2 (not 14 W/m^2)

Photon Energy Recycling Efficiency:

Total Light Energy on Panels Over Time:
Light Energy = Power × Time
Light Energy = 47 W × 20 hours
Light Energy = 47 W × 72,000 seconds
Light Energy = 3,384,000 J

Electrical Energy Output Over Time:
Electrical Energy = Panel Output Power × Time
Electrical Energy = 17.5 W × 20 hours
Electrical Energy = 17.5 W × 72,000 seconds
Electrical Energy = 1,260,000 J

Photon Energy Recycling Efficiency:
Recycling Efficiency = (Electrical Energy Output ÷ Light Energy Input) × 100
Recycling Efficiency = (1,260,000 J ÷ 3,384,000 J) × 100
Recycling Efficiency = 37.23%

3.8.2 Estimation of Energy Savings and Financial Benefits for Willis Tower with PV Installation

It is important to highlight that indoor light-activated PV systems are primarily designed for large public buildings, such as high-rises, where a substantial number of lights remain illuminated throughout the night for security purposes. In such buildings, lights often operate continuously, making it reasonable to assume a 24-hour daily operation. This constant availability of artificial light provides a distinct advantage for indoor PV systems, as their energy generation is unaffected by weather conditions or sunlight availability.

Below, we present an estimation of the potential energy savings achievable through indoor light-activated PVs when applied to a large-scale structure like the Willis Tower.

Given data for the Willis Tower with the installation of PVs:

- Total Floor Area: 418,000 m^2
- PV Panel Area: 30% of total floor area = 0.3 × 418,000 m^2 = 125,400 m^2
- LED Light Power Density: 5 W/m^2
- LED Operation: 24 hours/day
- PV Conversion Efficiency: 30%
- Number of Operating Days: 360 days/year
- Electricity Cost: $0.20 per kWh

To estimate the energy savings and financial benefits of installing indoor light-activated PV systems in Willis Tower, the following calculations are performed based on the provided data:

Total LED Power in the Building.

Total LED Power = LED Light Power Density × PV Panel Area

Total LED Power = 5 W/m^2 × 125,400 m^2 = 627,000 W = 627 kW

Total Energy Available to PVs per Day.

Daily Energy Available = Total LED Power × LED Operation Hours

Daily Energy Available = 627 kW × 24 hours = 15,048 kWh/day

Energy Generated by PVs per Day.

Energy Generated = Daily Energy Available × PV Conversion Efficiency

Energy Generated per Day = 15,048 kWh/day × 0.30 = 4,514.4 kWh/day

Annual Energy Generation.

Annual Energy = Energy Generated per Day × Number of Operating Days

Annual Energy = 4,514.4 kWh/day × 360 days = 1,625,184 kWh/year

Annual Cost Savings.

Cost Savings = Annual Energy × Electricity Cost

Cost Savings = 1,625,184 kWh/year × $0.20/kWh = $325,036.80/year

Summary of Results:

Total PV Panel Area: 125,400 m^2

Annual Energy Generation: 1,625,184 kWh/year

Annual Cost Savings: $325,036.80

The installation of indoor light-activated PV systems in Willis Tower demonstrates a practical solution for utilizing the "wasted" energy of LED lights that remain operational continuously. Generating over 1.6 GWh of electricity annually, the system reduces overall grid dependency and provides meaningful cost savings - estimated at approximately $325,000 per year based on a commercial electricity rate of $0.20/kWh. This approach reinforces the environmental viability of indoor PV systems and supports the broader goals of energy-neutral buildings and sustainable urban development, particularly in high-rise structures where lighting is a constant operational requirement.

These findings underscore the robustness of indoor PV systems across a range of realistic operating conditions, while also highlighting the current economic limitations of large-scale deployment. Nonetheless, the environmental benefits, combined with the potential for future cost reductions and integration with smart lighting and energy storage systems, suggest a promising role for indoor PV in next-generation sustainable building design. Future work should explore these integration pathways and assess lifecycle impacts to further refine the value proposition of indoor photovoltaic technologies.

4. Conclusions

This study demonstrates the strong potential of silicon-based photovoltaic (SPV) systems to harvest energy from indoor LED lighting with remarkably high efficiency. Under controlled conditions, a peak power conversion efficiency (PCE) of 31% was achieved at a distance of 0.8 m—approaching the Shockley–Queisser theoretical limit for silicon under solar illumination. This performance enhancement is attributed to the spectral alignment of LED emission with the silicon bandgap, along with reduced thermalization and reflection losses, and the directional, stable nature of LED lighting.

Systematic evaluation of SPV configurations revealed that both series and parallel arrangements can effectively optimize power output under low-intensity conditions. The observed photon recycling efficiencies exceeding 37% highlight the feasibility of reclaiming otherwise unused indoor lighting for meaningful energy generation. Extended operation under continuous illumination further confirms the reliability and practicality of such systems, particularly in urban environments such as high-rise buildings where artificial lighting is in near-constant use.

A case study applied to the Willis Tower projected annual energy generation exceeding 1.6 GWh, translating to potential electricity savings of over $325,000. While initial capital investment remains a consideration, sensitivity analyses suggest that advances in PV efficiency and rising electricity rates could substantially reduce payback time and improve overall sustainability outcomes. Moreover, the associated reduction in CO_2 emissions aligns well with goals for energy-neutral and carbon-conscious building design.

In conclusion, indoor light-driven PV systems present a promising, underutilized opportunity for decentralized, consistent, and environmentally responsible energy production. Future research should focus on elucidating the photophysical mechanisms behind high indoor PCEs, advancing cost-effective integration methods, and exploring synergies with smart lighting systems, building automation, and on-site energy storage to realize the full potential of next-generation sustainable building energy systems.

Acknowledgments

We gratefully acknowledge the financial support provided by the National Science Foundation (Grant No. CMMI-1953009) and the Michelman Green, Clean, and Sustainable Technology Research Innovation Program (F103484). We also acknowledge funding from the Swiss National Science Foundation (Project No. IZSEZ0_223270) for the project titled "Photo-Thermal Coating for Energy Efficient Windows."

Author Contributions

Conceptualization, D.S.; Data curation, A. K., T. M., M.S.G. and S.S.; Investigation, A.H., M. B., J.K., and D. S.; Project administration, D.S.; Resources, D.S. and A.H.; Supervision, D.S. All authors have read and agreed to the published version of the manuscript.

Competing Interests

The authors declare no conflict of interest.

Data Availability Statement

Data is available in a publicly accessible repository.

AI-Assisted Technologies Statement

We confirm that AI tools were used solely to assist with text polishing for readability, grammar, and error-free presentation. All scientific content, data, calculations, and interpretations were generated by the authors. We have carefully reviewed and edited all AI-assisted text to ensure accuracy and integrity, and we take full responsibility for the manuscript content.

References

1. Parida B, Iniyan S, Goic R. A review of solar photovoltaic technologies. Renew Sustain Energy Rev. 2011; 15: 1625-1636.
2. Poponi D. Analysis of diffusion paths for photovoltaic technology based on experience curves. Sol Energy. 2003; 74: 331-340.
3. Mehrtash M, Quesada G, Dutil Y, Rousse D. Performance evaluation of sun tracking photovoltaic systems in Canada. Proceedings of the 20th Annual International Conference on Mechanical Engineering-ISME2012; 2012 May 16-18; Shiraz, Iran.
4. Mondol JD, Yohanis YG, Norton B. The impact of array inclination and orientation on the performance of a grid-connected photovoltaic system. Renew Energy. 2007; 32: 118-140.
5. Fouad MM, Shihata LA, Morgan EI. An integrated review of factors influencing the perfomance of photovoltaic panels. Renew Sustain Energy Rev. 2017; 80: 1499-1511.
6. Ito M, Kato K, Sugihara H, Kichimi T, Song J, Kurokawa K. A preliminary study on potential for very large-scale photovoltaic power generation (VLS-PV) system in the Gobi Desert from economic and environmental viewpoints. Sol Energy Mater Sol Cells. 2003; 75: 507-517.

7. Che L, Li N, Wei W, Li J, Ji j, Zhao X, et al. Day–Night energy harvesting: Photovoltaics-driven moisture evaporation and absorption for simultaneous 24-hour power and dehumidification. Innov Energy. 2025; 2: 100078.
8. Wei W, Li N, Che L, Fan Y, Liu H, Ji J, et al. A continuous 24-hour power generated PV-TEG-PCM hybrid system enabled by solar diurnal photovoltaic/thermal conversion and nocturnal sky radiative cooling. Energy Convers Manag. 2024; 321: 119086.
9. Jäger-Waldau A. Snapshot of photovoltaics – March 2025. EPJ Photovolt. 2025; 16: 22.
10. Van de Ven DJ, Capellan-Peréz I, Arto I, Cazcarro I, De Castro C, et al. The potential land requirements and related land use change emissions of solar energy. Sci Rep. 2021; 11: 2907.
11. Montoya FG, Peña-García A, Juaidi A, Manzano-Agugliaro F. Indoor lighting techniques: An overview of evolution and new trends for energy saving. Energy Build. 2017; 140: 50-60.
12. Yun GY, Kim H, Kim JT. Effects of occupancy and lighting use patterns on lighting energy consumption. Energy Build. 2012; 46: 152-158.
13. Byun J, Hong I, Lee B, Park S. Intelligent household LED lighting system considering energy efficiency and user satisfaction. IEEE Trans Consum Electron. 2013; 59: 70-76.
14. Roisin B, Bodart M, Deneyer A, D'herdt P. Lighting energy savings in offices using different control systems and their real consumption. Energy Build. 2008; 40: 514-523.
15. Mirrahimi S, Mohamed MF, Haw LC, Ibrahim NL, Yusoff WF, Aflaki A. The effect of building envelope on the thermal comfort and energy saving for high-rise buildings in hot–humid climate. Renew Sustain Energy Rev. 2016; 53: 1508-1519.
16. Mostafavi F, Tahsildoost M, Zomorodian Z. Energy efficiency and carbon emission in high-rise buildings: A review (2005-2020). Build Environ. 2021; 206: 108329.
17. Cimini G, Freddi A, Ippoliti G, Monteriù A, Pirro M. A smart lighting system for visual comfort and energy savings in industrial and domestic use. Electr Power Compon Syst. 2015; 43: 1696-1706.
18. Yun GY, Jung H, Kim JT. Energy-saving potential of LED lighting systems. Indoor Built Environ. 2013; 22: 235-241.
19. Kıyak İ, Oral B, Topuz V. Smart indoor LED lighting design powered by hybrid renewable energy systems. Energy Build. 2017; 148: 342-347.
20. Chew I, Kalavally V, Oo NW, Parkkinen J. Design of an energy-saving controller for an intelligent LED lighting system. Energy Build. 2016; 120: 1-9.
21. Katepalli A, Wang Y, Shi D. Solar harvesting through multiple semi-transparent cadmium telluride solar panels for collective energy generation. Sol Energy. 2023; 264: 112047.
22. O'Kane M. Solar cell efficiency formula [Internet]. Ossila. Available from: https://www.ossila.com/pages/solar-cell-efficiency-formula#:~:text=PCE%20represents%20the%20conversion%20ratio,Short%20circuit%20current%20(JSC).
23. Wang Q, Xu B, Sun J, Liu H, Zhao Z, Yu D, et al. Direct band gap silicon allotropes. J Am Chem Soc. 2014; 136: 9826-9829.
24. Abdelhady S, Abd-Elhady MS, Fouad MM. An understanding of the operation of silicon photovoltaic panels. Energy Procedia. 2017; 113: 466-475.
25. Bagnall DM, Boreland M. Photovoltaic technologies. Energy Policy. 2008; 36: 4390-4396.
26. Sze SM, Ng KK. Charge-Coupled Device (CCD). In: Physics of Semiconductor Devices. 3rd ed. Hoboken, NJ: John Wiley & Sons; 2007. pp. 708-713.

27. Shockley W, Queisser HJ. Detailed balance limit of efficiency of p--n junction solar cells. J Appl Phys. 1961; 32: 510-519.
28. Takeda Y, Sato S, Morikawa T. Effects of impact ionization and Auger recombination on hot-carrier solar cells and hot-carrier photocatalysts. Jpn J Appl Phys. 2023; 62: SK1003.
29. Le Bris A, Rodiere J, Colin C, Collin S, Pelouard JL, Esteban R, et al. Hot carrier solar cells: Controlling thermalization in ultrathin devices. IEEE J Photovolt. 2012; 2: 506-511.
30. Strümpel C, McCann M, Beaucarne G, Arkhipov V, Slaoui A, Švrček V, et al. Modifying the solar spectrum to enhance silicon solar cell efficiency—An overview of available materials. Sol Energy Mater Sol Cells. 2007; 91: 238-249.
31. Takeguchi K, Nakayama K, Chantana J, Kawano Y, Nishimura T, Hishikawa Y, et al. Spectral gain and loss of different-type photovoltaic modules through average photon energy of various locations in Japan. Sol Energy. 2021; 214: 1-10.
32. Daxini R, Wu Y. Review of methods to account for the solar spectral influence on photovoltaic device performance. Energy. 2024; 286: 129461.
33. Hamadani BH. Understanding photovoltaic energy losses under indoor lighting conditions. Appl Phys Lett. 2020; 117: 043904.